The structure and properties of ribbon-shaped carbon fibers with high orientation

Guanming Yuan [a], Xuanke Li [a]*, Zhijun Dong [a], Aidan Westwood [b], Brian Rand [c], Zhengwei Cui [a], Ye Cong [a], Jiang Zhang [a], Yanjun Li [a], Zhongwei Zhang [d], Junshan Wang [d]

a Hubei Province Key Laboratory of Coal Conversion & New Carbon Materials, Wuhan University of Science and Technology, Wuhan 430081, China;

b Institute for Materials Research, University of Leeds, Leeds LS2 9JT, United Kingdom;

c SARChI Chair of Carbon Technology and Materials, Institute of Applied Materials, University of Pretoria, Pretoria 0002, South Africa;

d Aerospace Research Institute of Materials and Processing Technology, Beijing, 100076, China.

Abstract: Using a naphthalene-derived mesophase pitch as a starting material, highly oriented ribbon-shaped carbon fibers with a smooth and flat surface were prepared by melt-spinning, oxidative stabilization, carbonization and graphitization. The preferred orientation, morphology and microstructure, as well as physical properties, of the ribbon-shaped carbon fibers were characterized. The results show that, the ribbon-shaped fibers possessed uniform shrinkage upon heat treatment, thereby avoiding shrinkage cracking commonly observed in round-shaped fibers. As heat treatment progressed, the ribbon-shaped graphite fibers displayed larger crystallite sizes and higher orientation of

* Corresponding author. Tel.: Fax: +86 27 86556906
E-mail address: xkli8524@sina.com (X. Li)

graphene layers along the main surface of the ribbon-shaped fiber in comparison with corresponding round-shaped fibers. The stability of the ribbon-shaped graphite fibers towards thermal oxidation was significantly higher than that of K-1100 graphite fibers. The longitudinal thermal conductivity of the ribbon fibers increased, and electrical resistivity decreased, with increasing the heat treatment temperatures. The longitudinal electrical resistivity and the calculated thermal conductivity of the ribbon-shaped fibers graphitized at 3000 °C are about 1.1 μΩ m and above 1100 W/m K at room temperature, respectively. The tensile strength and Young's modulus of these fibers approach 2.53 and 842 GPa, respectively.

1. Introduction

Mesophase pitch-based carbon fiber has been recognized as a strategic material because of its higher Young's modulus and greater thermal and electrical conductivity compared with carbon fibers derived from polyacrylonitrile [1-3]. Its well-developed graphitic structure is known to be the origin of its superior stiffness and conductivity which is attractive for many applications; one example is in the thermal management field due to its excellent thermal transport properties [4-6]. The most thermally conductive, commercially available mesophase pitch-based graphite fiber, K-1100 (produced by BP-Amoco), has a nominal thermal conductivity value over 1000 W/m K [7]. This high value of thermal conductivity is a direct result of its highly crystalline graphitic structure and a high degree of orientation parallel to the fiber axis. However, preparing such small fibers with a uniform diameter of ~7 μm requires a complex combination of processing parameters [8], in particular precise control of the transverse

texture of the as-spun pitch fibers. It has been well documented that fibers with a radial transverse texture offer a high degree of graphitization and thermal conductivity [5]. However, open wedge cracks often are formed in fibers with radial transverse structure during their subsequent high temperature heat-treatment which may affect their final properties [9,10]. On the other hand, as-spun mesophase pitch fibers with larger diameters may be beneficial for development of a higher degree of preferred orientation of graphite crystals, but stabilization of these fibers requires a longer time compared with those of smaller diameters and some randomization of the crystal preferred orientation in the fibers often occurs [9,11,12]. Thus the diameters of carbon fibers that can be achieved in commercial processes are restricted by the time-consuming stabilization process. Therefore, carbon fibers with average diameters larger than 15 μm are rarely produced.

Ribbon-shaped carbon fibers can efficiently overcome the limitations imposed by crack formation and maximum diameter because, through the control of processing parameters, they can be made to possess a highly ordered structure with the basal plane layers oriented predominantly perpendicular [5,7] or parallel [7] to the main surface of the ribbon-shaped fiber. Previous research [7,13] indicates, qualitatively, that low shear rates in a slit-shaped die tend to cause alignment of the microstructure parallel to the tape axis and to the main surface of the tape, whereas higher shear rates tend to cause alignment parallel to the tape axis but approximately perpendicular to the main surface of the tape. In the case of low shear rates, the latter texture is also observed at the tape edges. Also, at least for low shear rates, the degree of misorientation in the microstructure is larger for wider tapes (i.e. from wider slit-shaped dies), although this disparity between wide and narrow tapes decreases with increasing heat treatment. The graphite crystal

orientation in a mesophase pitch-based ribbon fiber is superior parallel to the longitudinal direction of fiber, compared with that of traditional commercial round-shaped fibers [4,5]. This allows these ribbon-shaped fibers to be graphitized more easily than round-shaped fibers at lower graphitization temperatures, and hence with lower production costs. Ribbon-shaped fibers graphitized at only 2400 °C exhibit transport properties comparable to those of commercial round-shaped fibers graphitized at temperatures above 3000 °C [14]. Furthermore, ribbon-shaped carbon fibers can be made with large cross-sectional areas of ~200 times of those of conventional round-shaped carbon fibers [7] but their low thickness, perpendicular to the main fiber surface, offers a short diffusion pathway for oxygen, enabling the ribbon-shaped fibers to be easily stabilized in air or oxygen. It is well known that oxidative stabilization is diffusion-controlled over larger pathways [15]. In addition, for thicker round-shaped fibers in particular, the rate of reaction in the pitch not only becomes slower and slower with increasing distance from the interface between the pitch and the oxidizing atmosphere but, at high stabilization temperatures, it may be further hindered as the outer surface becomes stabilized rapidly and so becomes a diffusion barrier to deeper stabilization [12]. Thus the thickness of as-spun ribbon-shaped pitch fibers is commonly controlled so as to be less than 30 μm in order to achieve complete stabilization. Up to now, there are few reports detailing the structure and properties of ribbon-shaped carbon fibers with a large transverse area.

In this paper, highly oriented ribbon-shaped carbon fibers, with a smooth and flat surface, were prepared by melt spinning a naphthalene-derived mesophase pitch. The preferred orientation, morphology, microstructure and texture of the ribbon-shaped carbon fibers heat treated at various temperatures were then characterized. In particular,

the electrical and thermal transport properties, as well as the mechanical properties, of the ribbon-shaped fibers produced under various conditions are also reported.

2. Experimental

2.1 Preparation of ribbon-shaped pitch fibers

A commercial naphthalene-derived synthetic mesophase pitch produced by Mitsubishi Gas Chemical Corporation was used directly as a raw material for spinning of pitch fibers. This type of mesophase pitch is 100% anisotropic and has a softening point of 265 °C. Uniformly molten mesophase pitch was extruded under nitrogen pressure of ~0.2 MPa through a slit-shaped die with an aspect ratio of about 80 at a spinning temperature of 320~330 °C to form ribbon-shaped pitch fibers which were drawn and collected by winding onto a hexagonal rotating drum at a rotational speed of ~20 m/min.

2.2 Heat-treatment of the ribbon-shaped pitch fibers

The as-spun ribbon-shaped pitch fibers were stabilized at 240~250 °C for 10~20 h in a flowing oxygen atmosphere. High orientation of lamelliform molecules within the mesophase ribbons is achieved in the shear field within the spinnerette slot-shaped die as was demonstrated by Lu et al [9]. After complete stabilization (the formed oriented internal structure of the pitch fibers during the extrusion process was fixed so as not to relax or deform or even melt in the subsequent high temperature treatments), the stabilized ribbon fibers were heat treated at ~400 °C as a pre-carbonization step, and subsequently carbonized at 700, 800, 1000, 1300 and 1600 °C for 1 h under nitrogen atmosphere in a tube furnace using a heating rate of 1 °C/min. The carbonized fibers were finally graphitized at 2000, 2400, 2800 and 3000 °C at a heating rate of 15 °C/min for 15

min to obtain highly oriented ribbon fibers.

2.3 Microstructure and physical properties of the ribbon-shaped carbon fibers

The degree of structural orientation of the ribbon-shaped fiber samples carbonized at 1600 °C and graphitized at 3000 °C were determined by X-ray diffraction (XRD) analysis using Cu K_α radiation (λ = 0.15406 nm). For XRD of randomly oriented specimens, powder samples were prepared by crushing fibers with an agate mortar and pestle. The fiber powders were mounted on a flat glass sample holder. For XRD of equatorially oriented ribbon-shaped fibers, the fibers were straightened out and taped to a glass slide, covering about 2 cm^2 and ensuring that only one layer of the fibers was mounted on the glass slide aligned with their basal planes parallel to the glass (i.e. with their basal planes perpendicular to the incident X-ray beam). Mounting of the transverse section of ribbon-shaped fibers for an XRD meridional scan (i.e. with their transverse sections perpendicular to the incident X-ray beam) was difficult due to their relatively small cross section and fragile nature but this was achieved by mounting the ribbon fibers' end-on in a polyester resin block. The ribbon-shaped fibers were vertically cast into the resin block before curing with the cross-sections of the fibers parallel to the polishing surface.

Raman experiments of the ribbon-shaped fibers in powder form were performed on a Renishaw InVia 2000 Raman microscope using Ar^+ 514.5 nm radiation for excitation at a power of 25 mW. The testing ribbon-shaped fiber was ground into a fine powder with uniform grain size, and all measurements were carried out with the same sample orientation relative to the laser beam in order to reduce the influence due to any preferred orientation. These studies only probed the basal faces (as confirmed by the corresponding

XRD results) of the powdered samples and so the intensity ratio of the D and G peaks (I_D/I_G ratio) would not be expected to be sensitive to sample orientation (but the I_D/I_G ratio would, of course, be expected to reduce upon heat treatment to develop the graphitic structure).

The morphology and microstructure of the ribbon-shaped carbon fibers were imaged with a NOVA 400 NANO field emission scanning electron microscope (SEM). Polished cross-sections of the ribbon-shaped carbon fibers embedded in a block of polyester resin were observed under a Carl Zeiss AX10 polarized light microscope (PLM) in reflectance mode. Lattice fringe images of ribbon-shaped fibers were obtained using a JEM 2100F high resolution transmission electron microscope (HRTEM).

Thermogravimetric (TG) analyses of various fiber samples were performed on a STA 449/6/G TG analyzer under flowing air or nitrogen atmosphere from room temperature to 1000 °C at a heating rate of 10 °C/min.

The longitudinal electrical resistivities of the ribbon-shaped fibers heat treated at different temperatures were obtained by measurement averaging of ten individual ribbon-shaped fibers with a BS407 precision millimicro ohmmeter using a standard four-probe method at room temperature. The thermal conductivities of the ribbon-shaped fibers heat treated at various temperatures were calculated according to the three different formulae reported by Xing Zhang [16], Hiroshi Hara [17] and John Gerard Lavin [18]. These formulae were established based on a large quantity of experimental data about the relationship between electrical resistivity and thermal conductivity of various round-shaped carbon fibers derived from mesophase pitch. The empirical formulae used were also found to be good approximations for ribbon-shaped carbon fibers, which were

well-verified by Edie et al. [14] through two different measurement methods.

The tensile properties of the carbonized and graphitized ribbon-shaped fibers treated at various temperatures were measured by single-filament testing according to ASTM standard D3822-07 at a gauge length of 40 mm. About 30 ribbon-shaped fibers of each sample were tested. The broken tape ends were numbered and saved for transverse area measurements by using SEM and PLM.

3. Results and discussion

3.1 XRD and Raman analyses of the ribbon-shaped carbon fibers

Fig. 1(a) shows a diagram of three different methods (random scan, equatorial scan and meridional scan [19]) used for XRD characterization to determine the degree of structural orientation of ribbon-shaped fibers. The XRD profiles from the three different methods of analysis of the ribbon-shaped fibers, carbonized and graphitized at 1600 and 3000 °C, respectively, are shown in Fig. 1(b-d). The XRD random scan profiles show that the samples are pure carbon. There is one sharp diffraction at about $2\theta = 26.8°$ and another weak diffraction at roughly $2\theta = 54.7°$, which can be attributed to (0 0 2) and (0 0 4) crystal planes of hexagonal graphite but no other peaks are observed due to the highly directional orientation of the carbon layers in the samples. In comparison to the ribbon-shaped fibers carbonized at 1600 °C, the (0 0 2) diffraction intensity of ribbon-shaped graphite fibers of heat-treatment temperature (HTT) up to 3000 °C sharply increases due to the increase. This is again attributed to preferred orientation of the crystalline graphite layer in the ribbon-shaped fibers, as well as the increase of graphitization degree. The interlayer spacing ($d_{(002)}$) and microcrystal stacking height (Lc)

of the ribbon-shaped fibers graphitized at 3000 °C can reach 0.3356 and 26.77 nm (calculated by Scherrer formula), respectively. This value of d_{002} is very close to the theoretical value of 0.3354 nm for a single crystal graphite. The L_c value of such wide ribbon-shaped graphite fibers was larger than that of the narrow (20~30 μm) ribbon-shaped graphite fibers (whose L_c was only 13~14 nm) produced by Edie et al. [4]. The XRD equatorial scan profiles of the ribbon-shaped carbon and graphite fibers as shown in Fig. 1(c) indicates that one layer of flat ribbon-shaped fibers has the same diffraction peak position as those in Fig. 1(b) except for the appearance of new diffraction peaks resulting from the double-sided tape that was used. The (0 0 2) diffraction intensity of ribbon-shaped fibers graphitized at 3000 °C as shown in Fig. 1(b and c) is clearly different, while there seems no difference for that of ribbon-shaped fibers carbonized at 1600 °C. In comparison with Fig. 1(b and c), Fig. 1(d) shows a strong wide amorphous diffraction peak at $2\theta = 20.2°$ (attributed to the diffraction of the polyester resin that was used) and two diffraction peaks at about $2\theta = 42.4$ and 77.5° corresponding to the (1 0 0) and (1 1 0) crystal planes of carbon, which is consistent with the result reported by Hishiyama and Nakamura [20]. The (1 1 0) diffraction peak indicates the development of three-dimensional graphite stacking from the turbostratic structure in its carbon precursor. It is interesting to note that the strongest diffraction peak at $2\theta = 26.8°$ corresponding to the (0 0 2) crystal plane of hexagonal graphite, as shown in Fig. 1(b and c), completely disappears under the meridional diffraction scan. This indicates that all graphitic crystallites in the ribbon-shaped fiber are uniformly aligned in the direction perpendicular to the transverse section of resin block (i.e. crystal orientation parallel to the main surfaces of the ribbon-shaped fiber) [20,21].

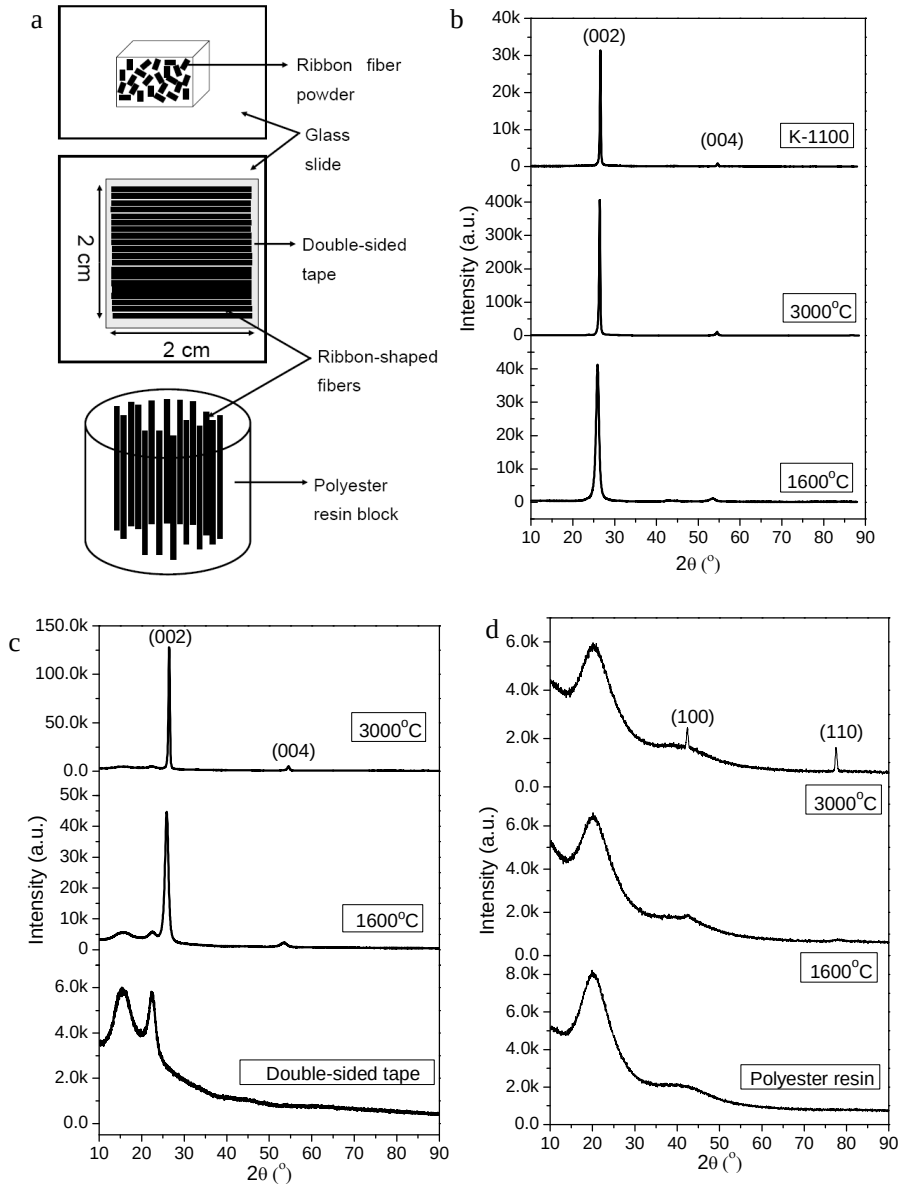

Fig. 1 (a) Diagram of a powdered form of ribbon-shaped fibers for the XRD random scan, a glass slide with one layer of ribbon-shaped fibers horizontally taped to it for the XRD equatorial scan and a columniform polyester resin block vertically embedded with ribbon-shaped fibers in the center for the XRD meridional scan, (b) XRD random diffraction scan patterns from fiber powders, (c) XRD equatorial scan patterns from ribbon-shaped fibers and (d) XRD meridional scan patterns of ribbon-shaped fibers.

The reason for the weakness of the (1 0 0) and (1 1 0) diffraction peaks observed for the ribbon-shaped fibers carbonized at 1600 °C may be the insufficient thickness of fibers embedded in the resin block or their relatively low graphitization degree. The significant difference between the XRD patterns as shown in Fig. 1(c and d) is attributed to the strong orientation of the (0 0 2) basal planes within the ribbon-shaped fibers. These results also show that the orientation of the (0 0 2) basal planes in the ribbon-shaped fibers is near perfect and the results are consistent with what would be predicted from the diagram of three X-ray scan preparation methods shown in Fig. 1(a).

Fig. 2 shows the typical first-order Raman spectra of the ribbon-shaped fibers heat treated at various temperatures. The Raman spectrum of K-1100 fibers is also provided for comparison purposes. The ribbon-shaped carbon fibers' D peak at about 1350 cm^{-1} and G peak at around 1580 cm^{-1} shown in Fig. 2(a) are both wide and intense, particularly for low heat treatment temperatures. The relatively high intensity of the D peak and the I_D/I_G ratio imply that the ribbon-shaped carbon fibers carbonized at 1000 °C show some disorder. In comparison to the ribbon-shaped fibers carbonized at 1000 °C, the D and G peaks of the ribbon-shaped fibers heat treated at 2000 °C as shown in Fig. 2(b) become more sharp and symmetric and both the intensity of the D-peak and the I_D/I_G ratio sharply decrease with the increase of HTT from 1000 to 2000 °C. This indicates an obvious decrease in defect and disordered carbon concentrations in the final product. The very weak D peak of ribbon-shaped fibers graphitized at 3000 °C shown in Fig. 2(c) is similar to that of K-1100 fibers shown in Fig. 2(d), which looks like that of stress-annealed pyrolytic graphite [22]. The I_D/I_G ratio of ribbon-shaped fibers

graphitized at 3000 °C is even lower than that of K-1100 fibers, and the calculated crystal coherence length (*L*a) values of the 3000 °C graphitized ribbon fibers and K-1100 fibers, according to the general equation (based on the intensity ratio of I_D/I_G) reported by Knight and White [23], are 34.2 and 16.9 nm, respectively, which indicates that a near-perfect crystal structure of graphite has formed in the ribbon-shaped graphite fibers.

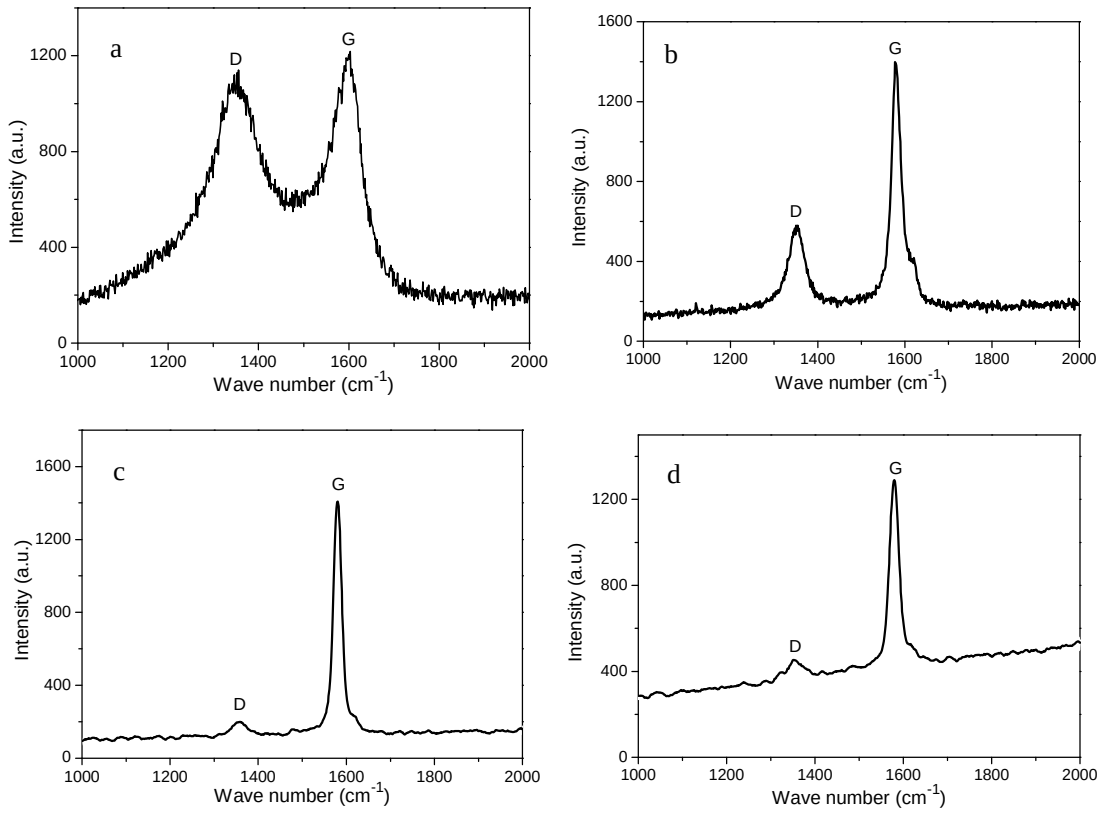

Fig. 2 Raman spectra of the ribbon-shaped fibers heat treated at (a) 1000, (b) 2000, (c) 3000 °C and (d) K-1100 fibers showing both D and G peaks.

3.2 Morphology and microstructures of the ribbon-shaped carbon fibers

Fig. 3(a) shows the typical optical photograph of the as-spun pitch fibers. It can be seen from Fig. 3(a) that the pitch fibers have uniform width, are black and shiny and were well

aligned on a flat plate of the hexagonal winding drum. The PLM photograph and SEM images shown in Fig. 3(b and c) show the transverse section of the ca. millimeter-wide ribbon-shaped pitch fibers heat treated at 400 °C.

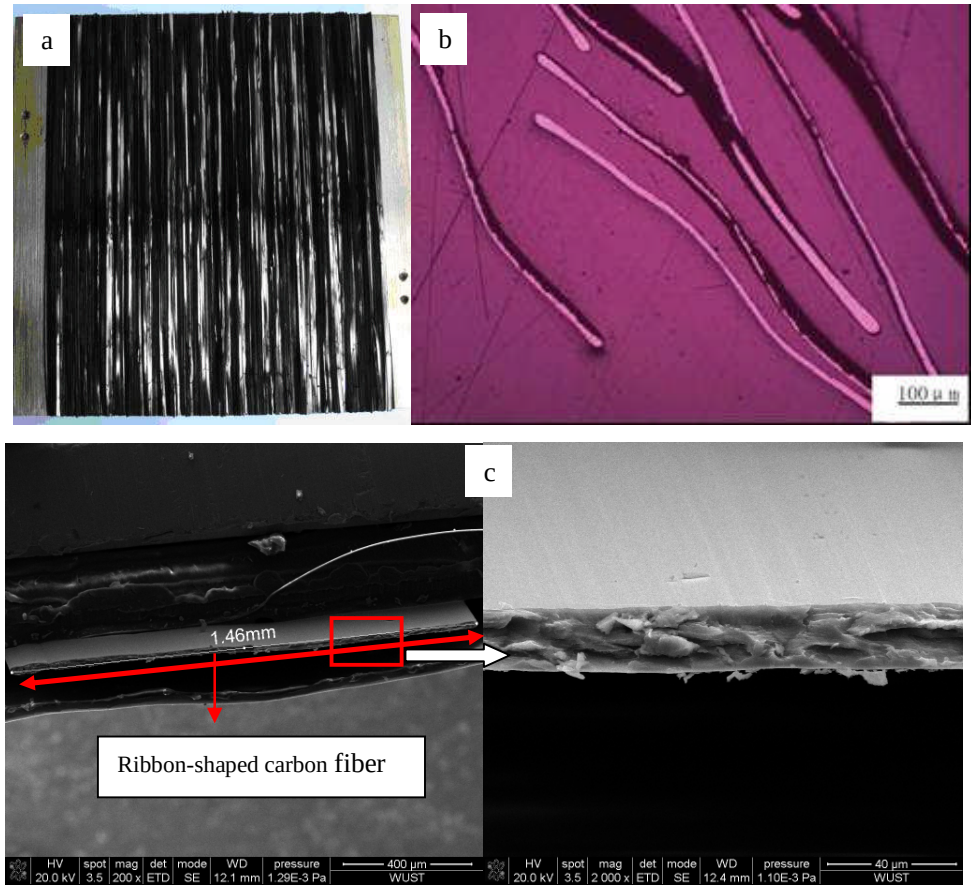

Fig. 3 Typical (a) optical photograph of well-aligned pitch fibers on a flat plate, (b) PLM micrograph and (c) SEM images of ribbon-shaped pitch fiber heat treated at 400 °C.

The images indicate that although these pitch fibers possess a uniform ribbon shape, the crystalline structure of ribbon fiber heat treated at such a low temperature, is very vague (similar to that of amorphous polymer) without evidence of distinct alignment of carbon layers as shown in Fig. 3(c). Their width and thickness were typically ~1.6 mm and ~22

μm, respectively, for the as-spun pitch fibers whist their cross-sectional area was found to be ~300 times that of conventional round-shaped carbon fibers with a diameter of ~8 μm.

Fig. 4 shows the PLM photographs of the transverse section of the carbonized and graphitized fibers. Different interference colour regions can be seen from the images, whereas the shape and size of microcrystal domains are difficult to distinguish. Fig. 4 (a-d) indicates that the ribbon fiber has a uniform thickness. Not much difference can be observed among the photographs except that the profile definition of the ribbon-shaped fiber gradually became clear with the increase of HTT. In comparison with the PLM photograph of ribbon-shaped fiber heat treated at a relatively low temperature (400 °C) as shown in Fig. 4(a), the graphitized ribbon-shaped fiber at 3000 °C, as shown in Fig. 4(d), displays clearly lamellar microstructure, which may suggest that a near-perfect alignment of oriented carbon layers parallel to the main surface of the ribbon fiber has been achieved. In contrast, there are some typical open wedge-shaped splitting textures as shown in Fig. 4(e) in the transverse sections of the round-shaped carbon fibers prepared from the same mesophase pitch by using a cylindrical die but otherwise similar process parameters, which may be caused by internal stresses within such highly anisotropic materials as the structure contracts during preferential orientation of crystallites in the fibers. Similarly the benchmark graphite fibers (K-1100) also formed an open wedge crack structure in the transverse section as shown Fig. 4(f), which is consistent with the scanning thermal microscopy images obtained by Blanco et al. [24].

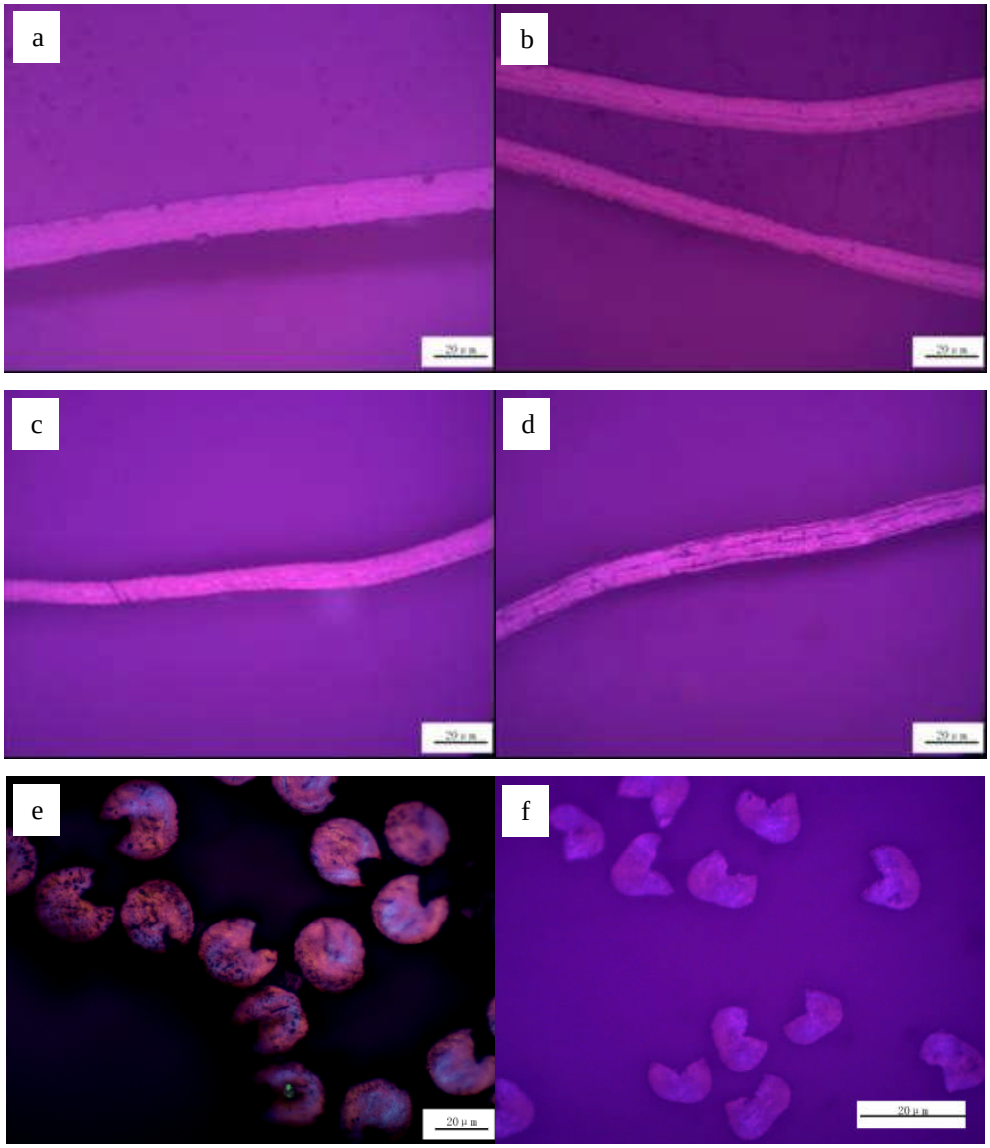

Fig. 4 Typical PLM photographs of transverse sections at the center of ribbon-shaped fibers heat-treated at (a) 400, (b) 1000, (c) 2000 and (d) 3000 °C, (e) round-shaped fibers with a diameter of ~20 μm carbonized at 1000 °C and (f) K-1100 fibers.

During carbonization and graphitization, the width and thickness of the ribbon-shaped fibers decreased from ~1.6 mm and ~22 μm for pitch fibers to ~1.2 mm (75% of original) and ~10 μm (45% of original) for graphitized fibers, respectively. However, the

ribbon-shaped fibers still maintain their ribbon shape, uniform thickness and continuous structural integrity without any damage as observed in Fig. 5(a and b). It can be seen from Fig. 5(c-f) that the growth and preferred orientation of graphite microcrystallites in the ribbon-shaped fibers are gradually improved with the increasing of HTTs. The crystalline structure of the ribbon fiber carbonized at 1000 °C as shown in Fig. 5(c) is markedly improved in comparison with that of the sample treated at 400 °C. The wave-shaped carbon layers have been formed, despite a few mismatches and voids in the ribbon fiber, owing to the strong decomposition and carbonization behavior in this temperature range. In comparison with the carbonized fiber as shown in Fig. 5(c and d), the graphitized fiber as shown in Fig. 5(e and f) displays better orientation of graphite layers parallel to the main surface of the ribbon fiber.

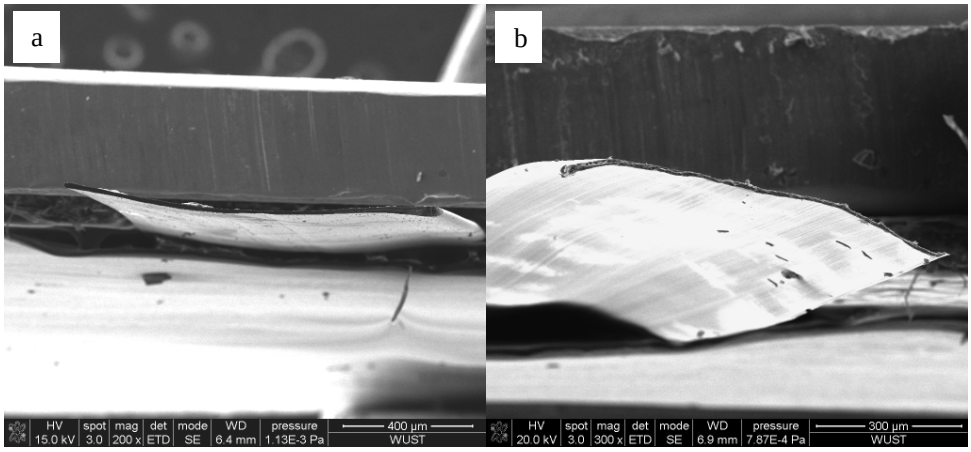

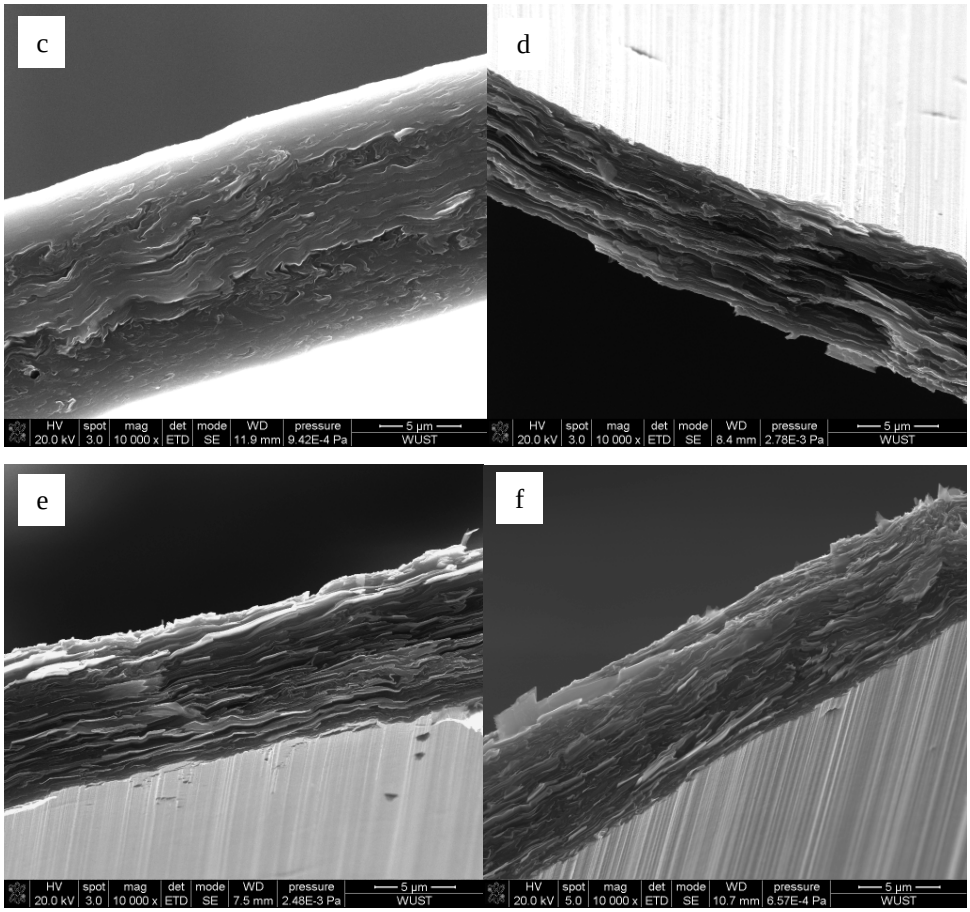

Fig. 5 Typical SEM images of a whole view of ribbon-shaped fibers (a) carbonized at 1000 °C and (b) graphitized at 3000 °C, and the transverse section at the center of ribbon-shaped fibers heat-treated at (c) 1000, (d) 1600, (e) 2800 and (f) 3000 °C.

The graphite crystals at edge sections of the ribbon-shaped fiber as shown in Fig. 6(a and b), show clear variations in crystal orientation, as compared to that of the center shown in Fig. 5(e). The SEM image from the center of the ribbon-shaped fiber in Fig. 5(e) shows a strong preferred orientation along the longitudinal direction and parallel to the main surface of the ribbon fibers. However, partial radial or wrinkled texture can be seen from Fig. 6(a and b), showing that the carbon layers at the two edges of the ribbon exhibit a preferred orientation along the longitudinal direction of the ribbon fiber and around the

edge outline in an oblique crossing pattern. The carbon layers at the center of the ribbon fiber display more perfect orientation than that of two edge sections. No crack from the edge to the center of the ribbon-fiber, even at the interfaces or connections of different crystal orientations, was observed.

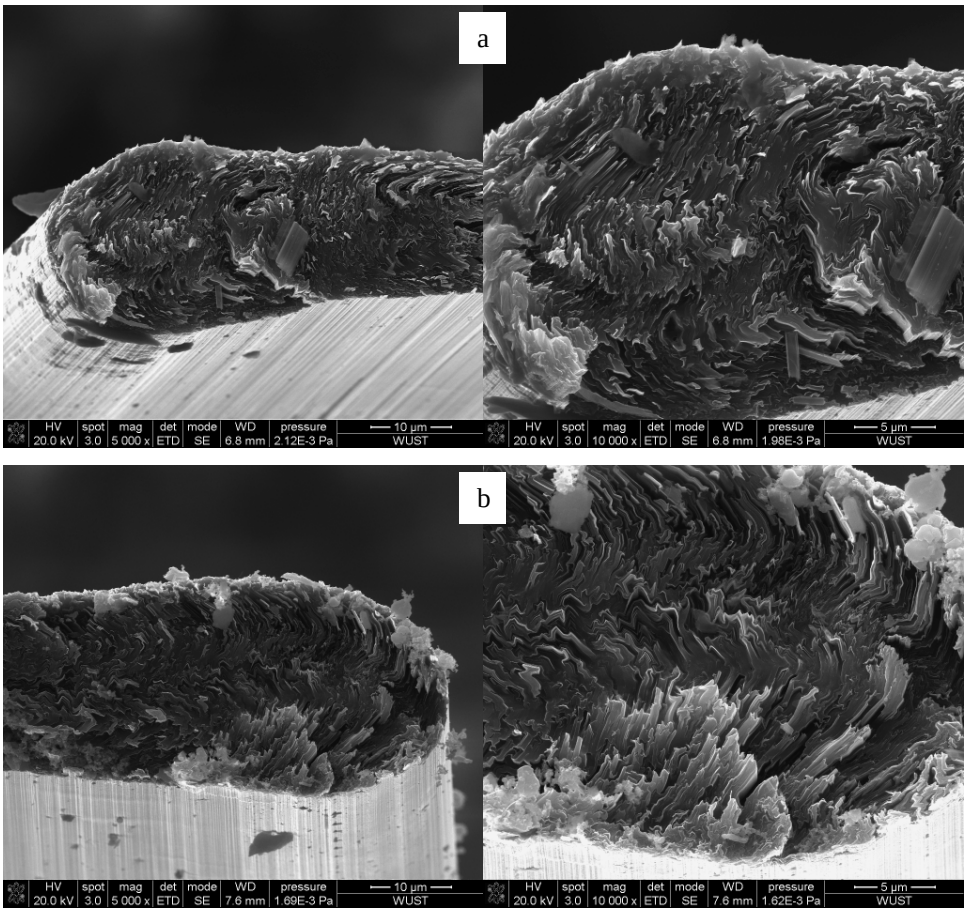

Fig. 6 Typical SEM images of the magnified transverse section at (a) left edge and (b) right edge of ribbon-shaped carbon fiber after graphitization at 2800 °C.

The obvious thickness difference (shown in Fig. 6 at a higher magnification) between the center and the edge of the ribbon fibers, after heat-treatment at 2800 °C, may have a close relation with the different crystal orientations in the two areas of the ribbon fibers. The

prepared ribbon-shaped carbon fibers seemingly possess more uniform morphology and higher crystal preferred orientation in comparison to the continuous mesophase pitch-based carbon tape with larger width (7.2 mm) and non-uniform thickness (10~30 μm) reported by Shinohara and Fujimoto [25]. By using a similar wider slit-shaped die, such crystal texture (with the basal plane layers oriented predominantly perpendicular to the main surface of the ribbon-shaped fiber) was also reported in references [7,13] by Rand et al.

It is interesting to note that round-shaped carbon fibers with a diameter of ~20 μm prepared from the same mesophase pitch, which display a radial or radial folded texture in their transverse sections as shown in Fig. 7(a), were easily split during the heat treatment process.

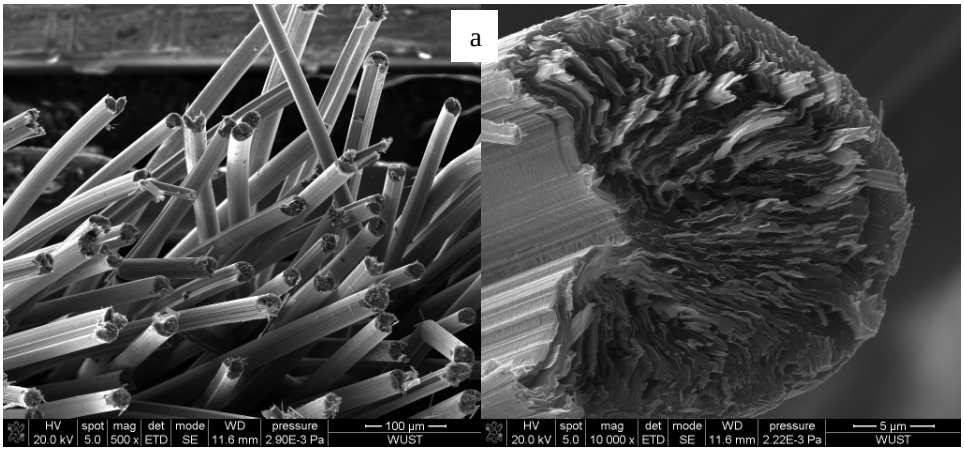

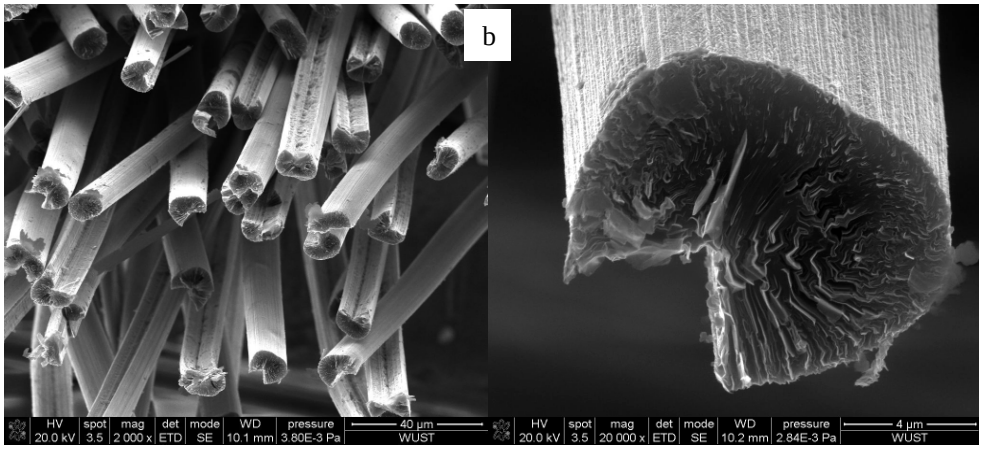

Fig. 7 Typical SEM images of round-shaped fibers (a) with a diameter of ~20 μm graphitized at 3000 °C and (b) K-1100 fibers.

This agrees well with the PLM observation result as shown in Fig. 4(e). K-1100 fibers also formed an open wedge crack structure as shown in Fig. 7(b), consistent with Fig. 4(f). Although such cracks can be reduced or eliminated by precise control of spinning [26], some round-shaped carbon fibers with a radial texture on the transverse section tend to split during the subsequent high-temperature heat treatment. By comparing the SEM images of ribbon-shaped graphite fibers and K-1100 fibers as shown in Fig. 5(e and f) and Fig. 7(b), respectively, it can be observed that ribbon-shaped graphite fibers possess more highly perfected crystal structure and greater layer orientation in comparison to the K-1100 fibers.

Typical HRTEM images of the ribbon-shaped carbon fibers and graphite fibers are shown in Fig. 8. It can be seen from the images in Fig. 8(a-e) that carbon nanocrystals in the ribbon-shaped fibers gradually grow and orient with the increase in HTT. The profile definition of the ribbon fiber also gradually became clear with increasing HTT. The higher the HTT, the greater the crystal sizes and orientation of the carbon crystallites,

resulting in anticipated significant increases in the electrical and thermal transport behaviour. The value of d_{002} (0.335 nm) observed from Fig. 8(e) was very close to the value of 0.3356 nm calculated from Scherrer analysis of the corresponding XRD pattern and to the theoretical value of 0.3354 nm for a single crystal graphite. The crystal size and degree of preferred orientation of ribbon-shaped fibers graphitized at 3000 °C observed from the HRTEM image as shown in Fig. 8(e) appear to be greater than those for the K-1100 fibers as shown in Fig. 8(f).

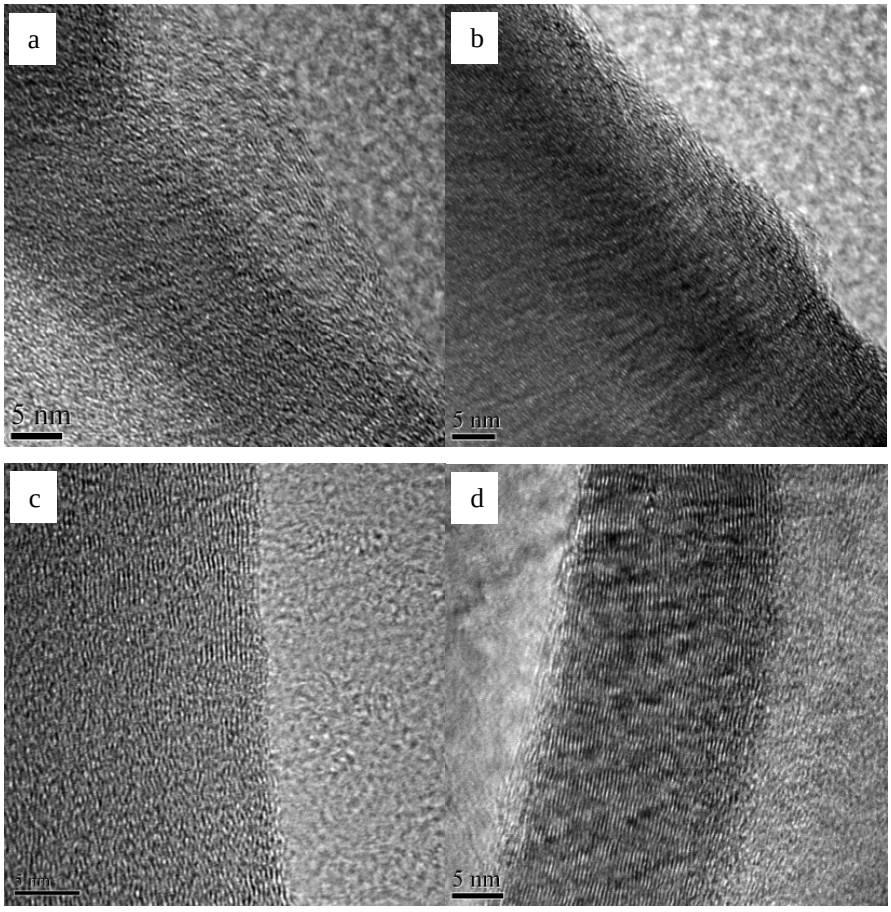

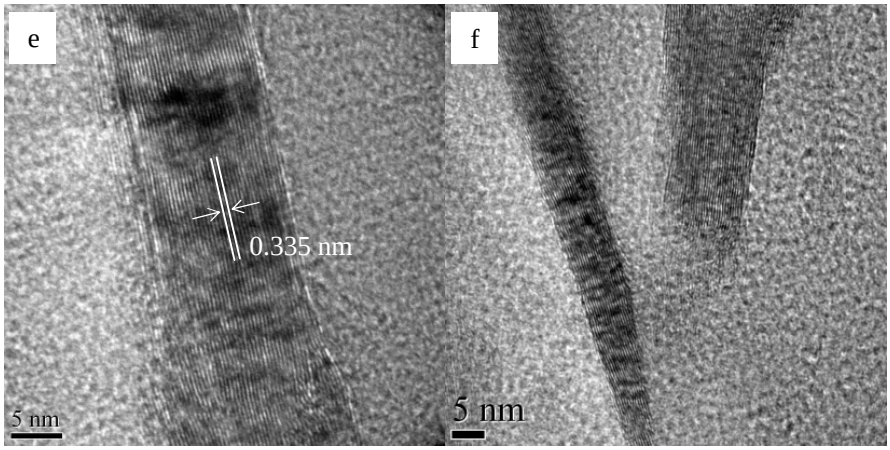

Fig. 8 Typical HRTEM images of the ribbon-shaped fibers heat treated at (a) 1000, (b) 1600, (c) 2000, (d) 2800, (e) 3000 °C and (f) K-1100 fibers.

It is generally known that the electrical and thermal properties of mesophase pitch-based carbon fibers have a close relation with their crystal structure and degree of preferred orientation [3,27]. Therefore, the electrical and thermal transport properties of the ribbon-shaped graphite fibers can be expected to be increased in comparison to both earlier narrow ribbon-shaped fibers [14] and K-1100 circular fibers [3].

3.3 TG analyses of the ribbon-shaped carbon fibers

The thermal behaviors of the as-spun pitch fibers under air or oxygen, and nitrogen atmospheres represent useful indicators of desired processing conditions for stabilization and carbonization. It is generally known that during the oxidation process, oxygen tends to react preferentially with aliphatic side groups. Therefore, the stabilization behaviors can be dependent on the concentration or flow rate of oxygen as well as on the reactivity of the pitch. This means that the higher the oxygen absorption, the more the aliphatic side groups in the pitch are oxidized, leading to accelerated stabilization. As shown in Fig. 9(a), oxygen uptake began at about 200 °C and combustion evidently started from

~350 °C in oxygen and ~440 °C in air. Thus, the optimum stabilization temperature range might be considered to be ca. 220~300 °C for such mesophase pitch. In comparison with an air atmosphere, the oxidation reaction was more acute in a pure oxygen atmosphere, meaning that the required oxidation temperature was relatively low and the oxidation period relatively short. The maximum weight gains in air and oxygen observed from the TG curves were about 2.0 and 4.0%, respectively. Under nitrogen atmosphere, weight loss started from 350 °C, and the residual weight remained approximately constant above 700 °C. The residual weight above 800 °C represents a carbon yield of ~77%, which is a higher carbon yield than polyacrylonitrile (~40%) and rayon (20~30%) under similar conditions [28].

Fig. 9(b) shows the TG curves of variously heat-treated mesophase pitch-based ribbon fibers and K-1100 fiber in air atmosphere. It can be seen from the curves of the carbon fibers heat treated at 1000 and 1600 °C that combustion began at about 550 and 600 °C, and that combustion was completed at about 780 and 820 °C, respectively. The thermal stability of the ribbon-shaped fibers heat treated at higher temperatures appeared to increase. The initial oxidation temperature of the ribbon-shaped fibers heat treated at 2000 °C was around 620 °C, increasing the onset temperature by about 70 °C in comparison to that of ribbon-shaped fibers heat treated at 1000 °C. With an increase in the graphitization temperature, the initial oxidation temperature shifts to higher temperature. For the ribbon-shaped fiber sample graphitized at 3000 °C, the initial oxidation temperature was about 700 °C, an increase of 150 °C in comparison with fibers heat treated at 1000 °C. Combustion of the 3000 °C ribbon fibers is complete at ca. 920 °C. This shows that the oxidation resistance of the ribbon-shaped fibers has a close

relation with the HTT. The higher the HTT, the more perfect the growth and orientation of the graphite crystals (which is demonstrated in the above microstructure analyses), resulting in lower concentrations of defects at which combustion can initiate and thus higher thermal stability and oxidation resistance. The thermal stability of ribbon-shaped graphitized fibers at 2800 and 3000 °C was significantly higher than that of K-1100 graphite fibers (even though these were graphitized at above 3000 °C [7,14]), which indicates that ribbon-shaped graphite fibers possess less defective crystal structure than K-1100 fibers.

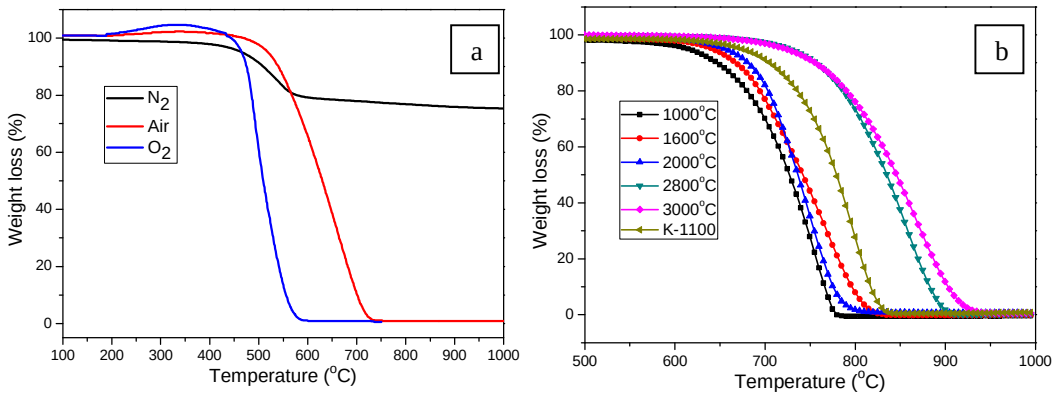

Fig. 9 The TG curves of (a) mesophase pitch fibers in nitrogen, air or oxygen atmospheres and (b) variously heat-treated mesophase pitch-based carbon ribbon fibers and K-1100 fiber in air atmosphere.

3.4 Electrical resistivities and thermal conductivities of the ribbon-shaped carbon fibers

Thermal conductivity testing of individual pitch-based carbon fibers is very difficult due to their small cross section and fragile nature [14]. Therefore, the thermal conductivities of the ribbon-shaped fibers, heat treated at various temperatures were

estimated according to the above mentioned three different formulae. The electrical resistivities of all ribbon-shaped fibers in the longitudinal direction of the fibers were measured at room-temperature using the standard four-probe method. Fig. 10 plots the values of electrical resistivity versus the corresponding calculated thermal conductivities. The electrical resistivity of the as-spun pitch fiber was similar to that of mesophase pitch, which is a typical electrical insulator as it displays electrical resistivities higher than 1.0×10^{12} Ω m [29]. The ribbon-shaped pitch fibers heat treated below 700 °C were also found to show very insulating behavior as their resistance values were beyond the measurable range (up to 20 KΩ) of the instrument used. The electrical resistivity of ribbon-shaped fibers heat treated at 700 °C was 1.01×10^{4} μΩ m. There appeared to be a large decrease in electrical resistivity when the fibers were heat treated from 700 to 800 °C. This sharp decrease in electrical resistivity can be attributed to the change in the structure of the fiber derived from mesophase pitch, which decomposes and carbonizes in this temperature range to become a continuous carbon, possessing a large number of mobile free electrons [30]. As can be seen from Fig. 10, the plot of electrical resistivities of the fibers heat treated to various temperatures, the electrical resistivity of ribbon-shaped fibers decreases to 42.93 μΩ m as the HTT reaches 800 °C. There was a further decrease in the electrical resistivity of the fiber samples upon heat treatment to 1000 °C, which was attributed to the complete transformation of the mesophase pitch or pitch coke to solid carbon [31].

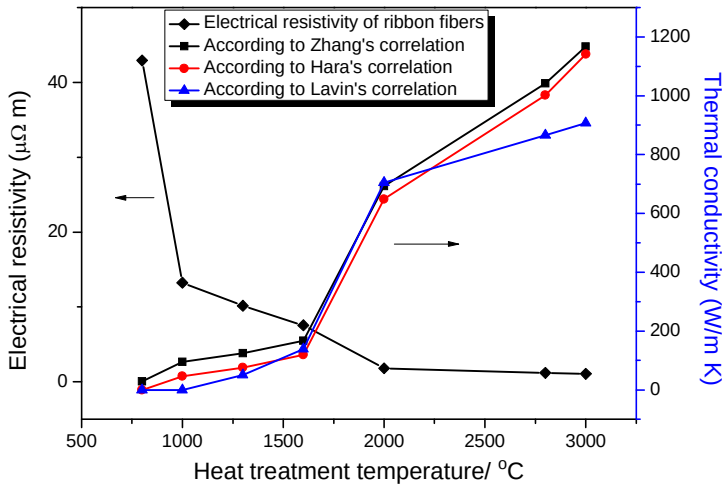

Fig. 10 The longitudinal electrical resistivities and calculated thermal conductivities of ribbon-shaped fibers heat treated at various temperatures. Thermal conductivities are calculated from the corresponding electrical resistivities according to Zhang's correlation, Hara's correlation and Lavin's correlation, respectively.

Upon further heat treatment of the ribbon-shaped fiber samples up to the graphitization temperature, the electrical resistivity of the samples decreases only slightly, due to the conversion of the carbon fibers to graphite fibers. The electrical resistivity of ribbon-shaped fibers graphitized at 3000 °C was found to be as low as 1.08 μΩ m. This value (within experimental limitations and errors) is close to the value for a single graphite flake in the in-plane direction, which lies in the range of 0.5~1.0 μΩ m [32]. In contrast, the axial electrical resistivity of K-1100 graphite fiber is about 1.17 μΩ m when measured in the same way and this agrees well with the reported value (1.1~1.3 μΩ m) [3].

The calculated thermal conductivities of the various ribbon-shaped fibers, as shown in Fig. 10, increase with the increase in HTT. The minimum and maximum values were

believed to be around 0~100 W/m K for the fiber samples heat treated below 1000 °C and 900~1100 W/m K for the fiber samples heat-treated above 2800 °C. However, the corresponding electrical resistivities of the fiber samples don't change much with increasing with HTT (especially above 2000 °C). The thermal conductivities of ribbon-shaped fibers graphitized at 3000 °C were around 1100 W/m K in the longitudinal fiber direction at room temperature. This result is in agreement with the thermal conductivity value of similar ribbon-shaped fibers, about 1000 W/m K, reported by Rand et al [33]. There was a significant increase in thermal conductivity with the increase of HTT from 1500 to 2000 °C. This is probably due to the mesophase pitch-based carbon fibers becoming strongly ordered, during heat treatment to 2000 °C, producing large crystallites with a completely lamellar stacking structure [34], as shown in the above microstructure analyses. Increases in HTT have been shown to result in improved perfection and preferred orientation of carbon crystallites and significant increases in the thermal conductivity [18,27]. The thermal conductivities of the ribbon-shaped fibers heat treated at various temperatures calculated according to the three formulae all have a similar rising trend and the results calculated by the correlations reported by Xing Zhang and Hiroshi Hara match very closely. The thermal conductivities at room-temperature (measured by a laser-flash diffusivity instrument LFA 457) along the longitudinal direction of the fibers in unidirectional ribbon-shaped fiber/carbon composites (prepared by using such ribbon-shaped carbon fibers as the filler and the same mesophase pitch powder as the binder) were ~10 and ~860 W/m K for a sample carbonized at 1000 °C and a sample graphitized at 3000 °C, respectively. Although lower than the values calculated for the individual fibers, the values measured by the laser flash technique are expected to

represent an underestimate of the true fiber thermal conductivity, when taking into account the composite density, volume fraction and possible misorientation of fibers in the composite, and thus they are consistent with the calculated values, which can therefore be considered reliable.

3.5 Mechanical properties of the ribbon-shaped carbon fibers

The mechanical properties of the carbonized and graphitized ribbon-shaped fibers are shown in Fig. 11. The tensile strength and Young's modulus of the ribbon-shaped fibers carbonized at 1000 °C are 876 MPa and 109 GPa, respectively. As the HTT increased to 2000 °C, the tensile strength and modulus of the ribbon-shaped fibers respectively increase to 1.28 and 276 GPa. These values are higher than those reported for the continuous mesophase pitch-based carbon tape with larger width (0.5 and 170 GPa) [25] due to the uniform thickness and better crystal orientation of the present ribbon-shaped fibers as well as to the increased risk of a critical flaw being present in the stressed volume of the wider tape. Upon further graphitization of the ribbon-shaped fiber samples up to 2400 °C, the tensile strength and modulus of the ribbon-shaped fibers markedly increase to 2.12 and 564 GPa. These values are larger than the corresponding values for previously reported graphitized narrow ribbon-shaped fibers (1.8~2.0 and 300~400 GPa) [35].

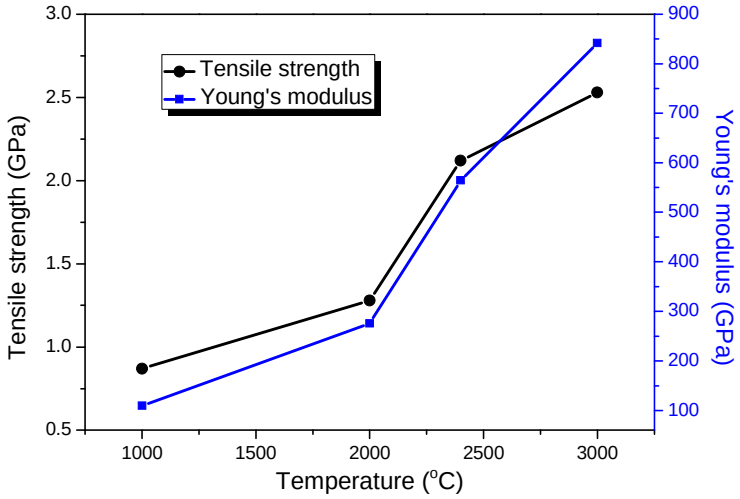

Fig. 11 The tensile strength and Young's modulus of ribbon-shaped fibers heat treated at various temperatures.

The ribbon-shaped fibers graphitized at 3000 °C show the highest tensile strength and modulus of approximately 2.53 and 842 GPa. Although these values are slightly lower than the corresponding values for K-1100 graphite fibers (3.1 and 965 GPa) [3], the strength of the ribbon-shaped fibers is high when taking into account their much larger cross-sectional area and the inevitable existence of a few flaws or holes in the ribbon fiber as well as the larger gauge length (40 mm instead of the standard 20 mm) in single-filament testing experiments, which all result in the decrease of mechanical properties. The high modulus of the ribbon-shaped graphite fibers is a direct result of the highly preferred orientation of the graphite crystal structure along the longitudinal direction of fiber.

4. Conclusions

Highly oriented ribbon-shaped carbon fibers with a smooth and flat surface were

prepared by melt-spinning, oxidative stabilization, carbonization and graphitization. XRD shows that graphite crystallites within the ribbon-shaped fibers develop upon progressive heat treatment, as confirmed by Raman spectroscopy, and are well aligned with their graphitic layers parallel to the main surfaces of the ribbon fiber (despite the differentia of crystal orientation at the center and edges of the ribbon fiber). SEM images show that the width and thickness of the ribbon-shaped fibers decreased from ~1.6 mm and ~22 μm for pitch fibers to ~1.2 mm and ~10 μm for graphitized fibers, respectively. In contrast to the mesophase pitch-based round fibers with radial texture in their transverse sections, which show wedge-shaped cracking behavior upon heat treatment, the ribbon-shaped fibers efficiently solve this crack problem through uniform shrinkage upon heat treatment and maintain their ribbon shape and structural integrity without any damage. Furthermore, ribbon-shaped graphite fibers possess more perfect crystal structure and layer orientation in comparison to round-shaped K-1100 fibers. The thermal stability towards oxidation of ribbon-shaped fibers graphitized at 2800 or 3000 °C is significantly higher than that of K-1100 fibers. With increasing HTT, of the ribbon-shaped fibers their electrical resistivity decreased and their thermal conductivity increased. The electrical resistivity and calculated thermal conductivity of the ribbon-shaped fibers graphitized at 3000 °C reach ~1.1 μΩ m and above 1100 W/m K, respectively, at room temperature in the longitudinal fiber direction, which compare favourably with K-1100 fiber. The strength and modulus of the ribbon-shaped fibers gradually increase with increasing HTT and the tensile strength and modulus of ribbon-shaped carbon fibers graphitized at 3000 °C reach 2.53 and 842 GPa, respectively. Although

slightly lower than that of K-1100 fiber, the strength of the ribbon fibers is high when taking into account their much larger cross-sectional area.

Acknowledgments

This work was sponsored by the Key Program of the Major Research Plan of the National Natural Science Foundation (grant No. 91016003) and the National Natural Science Foundation (grant No. 51372177) of China.

References

[1] Singer LS. Carbon fibers from mesophase pitch. Fuel 1981;60(9):839-47.

[2] Matsumoto T. Mesophase pitch and its carbon fibers. Pure & Applied Chem 1985;57(11):1553-62.

[3] Minus ML, Kumar S. The processing, properties, and structure of carbon fibers. J Microsc 2005;57(2):52-8.

[4] Edie DD, Robinson KE, Fleurot O, Jones SP, Fain CC. High thermal conductivity ribbon fibers from naphthalene-based mesophase. Carbon 1994;32(6):1045-54.

[5] Edie DD. The effect of processing on the structure and properties of carbon fibers. Carbon 1998;36(4):345-62.

[6] Adams PM, Katzman HA, Rellick GS, Stupian GW. Characterization of high thermal conductivity carbon fibers and a self-reinforced graphite panel. Carbon 1998;36(3):233-45.

[7] Lu SL, Blanco C, Appleyard S, Hammond C, Rand B. Texture studies of carbon and graphite tapes by XRD texture goniometry. J Mater Sci 2002;37(24):5283-90.

[8] Edie DD, Dunham MG. Melt spinning pitch-based carbon fibers. Carbon 1989;27(5):647-55.

[9] Lu SL, Blanco C, Rand B. Large diameter carbon fibres from mesophase pitch. Carbon 2002;40(12):2109-16.

[10] Mochida I, Yoon SH, Takano N, Fortin F, Korai Y, Yokogawa K. Microstructure of mesophase pitch-based carbon fiber and its control. Carbon 1996;34(8):941-56.

[11] Hamada T, Furuyama M, Sajiki Y, Tomioka T, Endo M. Preferred orientation of pitch precursor fibers. J Mater Res 1990;5(6):1271-80.

[12] Blanco C, Lu SL, Appleyard SP, Rand B. The stabilisation of carbon fibres studied by micro-thermal analysis. Carbon 2003;41(1):165-71.

[13] Galanopoulos E, Rand B, Westwood A. Wide, highly oriented mesophase pitch-based carbon tapes and their laminates. Extended abstracts, an International Conference on Carbon 2003. Oviedo (Spain): Spanish Carbon Society, 2003; P. 1-4.

[14] Gallego NC, Edie DD, Nysten B, Issi JP, Treleaven JW, Deshpande GV. The thermal conductivity of ribbon-shaped carbon fibers. Carbon 2000;38(7):1003-10.

[15] Singer LS, Mitchell S. Diffusion of oxygen into pitch. Carbon 1997;35(5):599-604.

[16] Zhang X, Fujiwara S, Fujii M. Measurement of thermal conductivity and electrical resistivity of a single carbon fiber. Int J Thermophys 2000;21(4):965-80.

[17] Hara H, Hirata M, Ban T. Carbon fiber composite sheet, use thereof as a heat conductor and pitch-based carbon fiber web sheet for use in the same. US patent 20090061193, 2009.

[18] Lavin JG, Boyington DR, Lahijani J, Nystem B, Issi JP. The correlation of thermal conductivity with electrical resistivity in mesophase pitch-based carbon fiber. Carbon

1993;31(6):1001-2.

[19] Liu YD, Chae HG, Kumar S. Gel-spun carbon nanotubes/polyacrylonitrile composite fibers. Part I: Effect of carbon nanotubes on stabilization. Carbon 2011;49(13): 4466-76.

[20] Hishiyama Y, Nakamura M. X-ray diffraction in oriented carbon films with turbostratic structure. Carbon 1995;33(10):1399-403.

[21] Chen GH, Wang HQ, Zhao WF. Fabrication of highly ordered polymer/graphite flake composite with eminent anisotropic electrical property. Poly Adv Technol 2008;19(8):1113-7.

[22] Tuinstra F, Koenig JL. Raman spectrum of graphite. J Chem Phys 1970;53(3): 1126-30.

[23] Knight DS, White WB. Characterization of diamond films by Raman spectroscopy. J Mater Res, 1989;4(2):385-93.

[24] Blanco C, Appleyard SP, Rand B. Study of carbon fibres and carbon–carbon composites by scanning thermal microscopy. J Microsc 2002;205(1):21-32.

[25] Shinohara K, Fujimoto H. The microstructure of highly-oriented graphite tape prepared from mesophase pitch by melt-blowing. Carbon 2012;50(13):4926-31.

[26] Yoon SH, Takano N, Korai Y, Mochida I. Crack formation in mesophase pitch-based carbon fibres: Part I some influential factors for crack formation. J Mater Sci 1997;32(10):2753-8.

[27] Gallego NC, Edie DD. Structure-property relationships for high thermal conductivity carbon fibers. Compos A 2001;32(8):1038-43.

[28] Huang XS. Fabrication and properties of carbon fibers. Mater 2009;2(4):2369-403.

[29] Sharp JA. Electrical resistivity of pitch during heat treatment. Fuel 1987;66(11):1487-90.

[30] Dumont M, Dourges MA, Bourrat X, Pailler R, Naslain R, Babot O, et al. Carbonization behavior of modified synthetic mesophase pitches. Carbon 2005;43(11):2277-84.

[31] Marsh H, Menendez R. Carbons from pyrolysis of pitches, coals, and their blends. Fuel Process Technol 1988;20(1-3): 269-96.

[32] Dutta AK. Electrical conductivity of single crystals of graphite. Phys Rev 1953;90(2):187-92.

[33] Rand B, Lu SL, Blanco C, Daniels H, Brydson RMD. Structure and properties of highly oriented mesophase graphite tapes of high conductivity. Extended abstracts, an International Conference on Carbon 2002. Beijing (China): Chinese Carbon Society, 2002; P. 1-4.

[34] Horr NE, Bourgerette C, Oberlin A. Mesophase powders (carbonization and graphitization). Carbon 1994;32(6):1035-44.

[35] Edie DD, Fain CC, Robinson KE, Harper AM, Rogers DK. Ribbon-shape carbon fibers for thermal management. Carbon 1993;31(6):941-9.

List of captions for Figures

Fig. 1 (a) Diagram of a powdered form of ribbon-shaped fibers for the XRD random scan, a glass slide with one layer of ribbon-shaped fibers horizontally taped to it for the XRD equatorial scan and a columniform polyester resin block vertically embedded with ribbon-shaped fibers in the center for the XRD meridional scan, (b) XRD random diffraction scan patterns from fiber powders, (c) XRD equatorial scan patterns from ribbon-shaped fibers and (d) XRD meridional scan patterns of ribbon-shaped fibers.

Fig. 2 Raman spectra of the ribbon-shaped fibers heat treated at (a) 1000, (b) 2000, (c) 3000 °C and (d) K-1100 fibers showing both D and G peaks.

Fig. 3 Typical (a) optical photograph of well-aligned pitch fibers on a flat plate, (b) PLM micrograph and (c) SEM images of ribbon-shaped pitch fiber heat treated at 400 °C.

Fig. 4 Typical PLM photographs of transverse sections at the center of ribbon-shaped fibers heat-treated at (a) 400, (b) 1000, (c) 2000 and (d) 3000 °C, (e) round-shaped fibers with a diameter of ~20 μm carbonized at 1000 °C and (f) K-1100 fibers.

Fig. 5 Typical SEM images of ribbon-shaped fibers (a) carbonized at 1000 °C and (b) graphitized at 3000 °C, and the transverse section at the center of ribbon-shaped fibers heat-treated at (c) 1000, (d) 1600, (e) 2800 and (f) 3000 °C.

Fig. 6 Typical SEM images of the magnified transverse section at (a) left edge and (b) right edge of ribbon-shaped carbon fiber after graphitization at 2800 °C.

Fig. 7 Typical SEM images of round-shaped fibers (a) with a diameter of ~20 μm graphitized at 3000 °C and (b) K-1100 fibers.

Fig. 8 Typical HRTEM images of the ribbon-shaped fibers heat treated at (a) 1000, (b) 1600, (c) 2000, (d) 2800, (e) 3000 °C and (f) K-1100 fibers.

Fig. 9 The TG curves of (a) mesophase pitch fibers in nitrogen, air or oxygen atmospheres and (b) variously heat-treated mesophase pitch-based carbon ribbon fibers and K-1100 fiber in air atmosphere.

Fig. 10 The longitudinal electrical resistivities and calculated thermal conductivities of ribbon-shaped fibers heat treated at various temperatures. Thermal conductivities are calculated from the corresponding electrical resistivities according to Zhang’s correlation, Hara’s correlation and Lavin's correlation, respectively.

Fig. 11 The tensile strength and Young’s modulus of ribbon-shaped fibers heat treated at various temperatures.